Stabilization of needle-crystals in the symmetric model of solidification

Claude-Alain Pillet

UNIVERSITÉ DE GENÈVE

SCHOLA GENEVENSIS MDLIX

STABILIZATION OF NEEDLE-CRYSTALS IN THE SYMMETRIC MODEL OF SOLIDIFICATION

C.-A. PILLET

Département de Physique Théorique

Université de Genève

CH-1211 Geneva 4, Switzerland

Abstract. We present the results of a careful numerical analysis of the stability problem for stationary needle-crystal solutions of the symmetric model of dentritic solidification. The major outcome is that such needle crystals are stable, at least on a time scale relevant to side-branching phenomena. Our study also indicates that the tip of the needle-crystal is very sensitive to external noises, thus supporting the selective amplification mecanism advocated by Langer, Barbieri and Barber [BBL] on the basis of a WKB analysis.

1. INTRODUCTION

In a preceding paper ([P]) we started a linear stability analysis of needle-crystals, and proved their stability with respect to side-branching modes by explicitly computing the essential spectrum of the linearized evolution equation of the symmetric model of Langer and Tursky (see [LT]). In this paper, which is a natural continuation of the first one, we concentrate on the other type of excitations of needle-crystals: the tip-splitting modes corresponding to discrete eigenvalues of the linear evolution operator. In contrast with the essential spectrum, this eigenvalues depend on the precise shape of the stationary solution as well as on detailed properties of the evolution equation. Except perhaps in the vanishing surface tension limit, where an asymptotic WKB approach is possible (see for example [BBL] and [BPS] for a heuristic development), an analytical treatment of this problem seems quite hopeless at the present time. Therefore we shall resort to numerical methods.

Of course a number of numerical works on various models of dentritic solidification have already been published, most of them based on a direct solution of the relevant evolution equation. However, and despite of the important theoretical interest of this problem, we are only aware of two numerical studies of the linear stability of non-local models ([LM] and [KL]). Unfortunately these two works lead to quite different results, in particular the conclusions of the first one is not compatible with the stability of side-branching modes. This discrepancy, and our need for a definite answer to the stability question, motivated this new numerical computation.

As a by-product of our calculations we also computed the linear response of the needle-crystal to time-periodic external perturbations. We are thus able to compare our results to the qualitative predictions of the WKB analysis in [BBL].

Although we do not provide our results with rigorous error bounds, we have been extremely careful in setting up the computation scheme and choosing the numerical algorithms. We have avoided any uncontrolled approximation, in particular we eliminated the need to compute continuum "eigenfunctions" which, being delocalized, are much to sensitive to boundary effects induced by truncation. We also gave up the usual quasi-stationary approximation which introduces a fake singularity at small momentum. All the numerical routines we used were extensively checked for numerical stability and accuracy. Each of them was then provided with a run-time stability test enabling a

global control on individual computations. Of course all computations were done in double precision arithmetics, and register accumulators used for matrix algebra. As a result we believe that the only remaining source of relevant errors is discretization. However we made a rudimentary numerical analysis of the continuum limit which gave good evidence for the discretization errors to be unimportant, as far as our conclusions are concerned.

2. RESULTS

In the two dimensional symmetric model we consider a needle-crystal moving with velocity v in the y-direction. We measure lengths in units of ρ, the radius of curvature of the tip, and times in units of ρ/v. Assuming this stationary front to be given by the graph

$$y = t - \phi(x),$$

we can write the linearized evolution equation for the normal deviation u from thr stationary shape as a function of an external perturbation q in the form

$$-\sigma\partial_s^2 u(s,t) - \sigma\kappa_0^2(s)u(s,t) - j_0^{\perp}(s)u(s,t) + (\Lambda u)(s,t) = q(s,t),$$

where s is the arclength down the stationary needle, κ_0 its curvature and $j_0^{\perp}$ the heat flux trough it. The integral operator Λ is further defined by

$$(\Lambda u)(s,t) \equiv \int_0^{\infty} \frac{d\tau}{2\pi\tau} \int_{-\infty}^{\infty} ds' \, \mathrm{e}^{-p\left[(X(s)-X(s'))^2+(\tau-\phi(X(s))+\phi(X(s')))^2\right]/2\tau} \left\{ p\left(1 - \frac{\phi(X(s)) - \phi(X(s'))}{\tau}\right) u(s', t-\tau) + \partial_t u(s', t-\tau) \right\},$$

where $X(s)$ is the x coordinate as a function of the arclength on the needle.

Since our main interest is in understanding the side-branching mechanism we decide to fix the physical parameters of the needle-crystal in all our calculations to some values close the ones given in [BBL] i.e.,

$$p = 0.05,$$
$$\sigma = 0.025.$$

At such a low value of σ the deviation from Ivantsov's parabola is so small that we may perfectly well neglect it (see for example [LM]). We also neglect the anisotropy of surface tension which is generally so tiny that its only relevance is in the velocity selection mechanism. Finally we may restrict our calculations to the subspace of functions which are symmetric with respect to the tip. Since the short time behavior of dendrites never shows any kind of anti-symmetry we have no reason to believe that the anti-symmetric sector could be more unstable than the symmetric one.

On the other hand we do not make the usual quasi-stationary approximation which is much more difficult to control. This regularizes the linearized evolution equation, but unfortunately makes its structure much more involved. For a time periodic external perturbation $qe^{i\omega t}$ of frequency ω, the linear response of the crystal $ue^{i\omega t}$ is easily seen to satisfy an equation of the following form

$$\hat{A}(\omega)u = q. \tag{2.1}$$

In the quasi-stationary approximation the operator $\hat{A}(\omega)$ is linear in ω, thus the stability of equation (2.1) is simply determined by solving a generalized eigenvalue problem. Without quasi-stationary approximation however, $\hat{A}(\omega)$ becomes non-linear in ω, therefore the stability analysis requires finding all values of ω in the lower half-plane for which the operator $\hat{A}(\omega)$ has a zero eigenvalue.

To understand our first result let us have a look at the complex ω plane in figure 1 (this is really a picture of the ω/p-plane). Unstable modes live in the lower half-plane. The upper curve is taken from [P] and is the boundary of the domain where $\hat{A}(\omega)$ is Fredholm. This means that for ω below this curve, zero can only be in the spectrum of $\hat{A}(\omega)$ if it is one of its isolated eigenvalue. The lower curve is the boundary of the set of ω for which the pseudo-differential symbol

$$\begin{aligned} a(\omega; s, \xi) &\equiv \mathrm{e}^{-i\xi s/\sqrt{\sigma}} \left(\hat{A}(\omega) \mathrm{e}^{i\xi \cdot/\sqrt{\sigma}} \right)(s) \\ &= \xi^2 - j_0^{\perp}(s) + \frac{i(\nu + \eta(s)\xi)}{\sqrt{\xi^2 + 2ip\sqrt{\sigma}(\nu + \eta(s)\xi)}} + \mathrm{O}(\sqrt{\sigma}) \end{aligned}$$

of $\hat{A}(\omega)$ admits a zero for some real (s, ξ). The following notation was used:

$$\nu \equiv \frac{\omega}{p},$$

$$\eta(s) \equiv \left(\frac{\phi'}{\sqrt{1 + \phi'^2}} \right) \circ X(s).$$

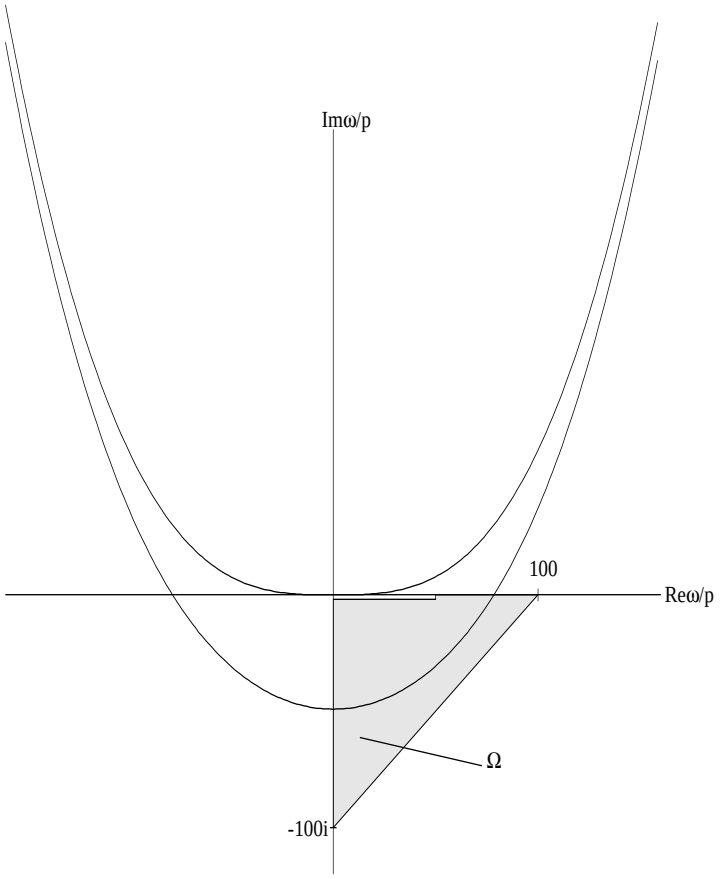

Fig. 1: the explored region Ω of the ω plane.

Thus we expect the values of ω for which $\hat{A}(\omega)$ has a zero eigenvalue to be roughly (i.e., to $O(\sigma^{1/2})$) localized between the two curves of figure 1. Taking into account the fact that, since $\hat{A}(-\bar{\omega}) = \hat{A}(\omega)^*$, the ω plane is symmetric with respect to its imaginary axis, it suffices to consider the right half plane. Our result is that for ω in the shaded area Ω in the figure, the eigenvalues of $\hat{A}(\omega)$ are bounded away from zero. Therefore, except possibly in the narrow strip

$$\{\omega \mid |\mathrm{Re}\omega| < 50p;\ -2p < \mathrm{Im}\omega < 0\}\,, \tag{2.2}$$

there is no unstable tip-splitting mode. Let us make some comments about this strip. Clearly any numerical calculation of the spectrum of $\hat{A}(\omega)$ will not resolve isolated eigenvalues which are too close to the essential spectrum because the corresponding

eigenfunctions will have a very long localization length, thus such a security region is inherent to the problem and can not be avoided. On the other hand if a zero eigenvalue would exists in this region, the resulting instability would have a very long characteristic time. In our case, such an instability would manifest itself after a period of the order of $\bar{\tau} = 100$ in the natural time unit of the crystal. This is typically of the same order of magnitude than the total observation time of a dendrite in a real experiment, and thus should not be relevant to side-branching. As a comparison the time corresponding to the critical frequency of [BBL] is $T_c \sim 4 << \bar{\tau}$. We are thus able to confirm that, at least in the considered regime, needle crystals are stable and that side-branching is not due to a global instability of the stationary solution.

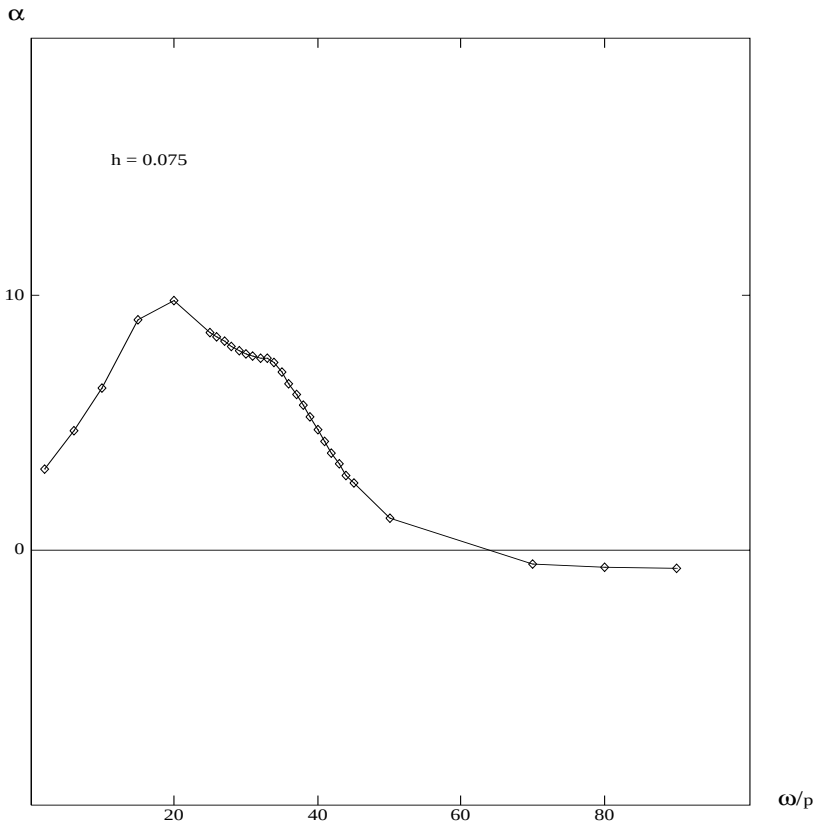

Fig. 2: the amplification rate α as a function of the real frequency ω.

Our second result concerns what we should call the local instability of equation (2.1). This is the fact that, as the WKB calculation of [BBL] shows, there is a whole band

I^u of frequencies for which the response to an external perturbation is exponentially large. More precisely for $\omega \in I^u$ and a perturbation q localized near the tip of the crystal, the solution u of equation (2.1) satisfies

$$W_0 \equiv \lim_{\sigma \to 0} \sigma^{1/2} \log |u| > 0$$

in some bounded region of the crystal side. We computed the linear response of the crystal to a sharply localized perturbation for values of the frequency ω between $2p$ and $90p$ (see section 4 for the precise shape of this perturbation). A look at figure 2, which shows the amplification rate

$$\alpha \equiv \log_{10}(\max_s |u(s)|)$$

as a function of the frequency, clearly reveals a very strong local instability with an amplification factor of up to 10^10. The unstable band can be estimated to be

$$[-60p, 60p] \subset I^u \subset [-70p, 70p],$$

in good qualitative agreement with the results of [BBL] (which are at $p = 0$). In particular their critical frequency which is $\omega_c \approx 48p$ in our units is well contained in I^u. This strongly support the idea of Langer (see [BBL]) that side-branching occurs as a selected amplification of noise at the tip of the dendrite.

3. MATHEMATICAL DETAILS

For computational as well as numerical reasons we will not work with the arclength parameter s, but rather with the x coordinate. We thus avoid the computation of the inverse arclength function $X(s)$. The important point however is that a uniformly spaced array of points on the x-axis generates, in a quick and easy way, a non-uniform discretization mesh on the needle. This mesh turns out to be well adapted to the the problem since it is dense (approximately uniformly spaced) near the tip where the operator is rapidly varying, and becomes looser on the sides where it is almost independent of x. Thus for a given number of discretization points we can combine the advantages of a small effective mesh-size at the tip and a large spatial cutoff.

The unitary map from $L^2(dx)$ to $L^2(ds)$ is easily seen to be given by

$$v(x) \mapsto u(s) \equiv \left[\left(1 + \phi'^2\right)^{-1/4} v \right] \circ X(s),$$

and to transform the operator $\hat{A}(\omega)$ into

$$\hat{A}(\omega) = -\sigma\,\partial_x \frac{1}{1+\phi'(x)^2}\partial_x + V(x) + \hat{\Lambda}(\omega),$$

where the potential V is given by

$$V \equiv -j_0^{\perp} - \frac{\sigma}{2}\left(\frac{1+\frac{5}{2}\phi'^2}{(1+\phi'^2)^3}\,\phi''^2 - \frac{\phi'\phi'''}{(1+\phi'^2)^2}\right),$$

and the integral operator $\hat{\Lambda}(\omega)$ has the kernel

$$\begin{aligned}
&\hat{\Lambda}(\omega; x, y) \equiv \\
&\int_0^{\infty} \frac{d\tau}{2\pi\tau}\, \mathrm{e}^{-p[(x-y)^2+(\tau-\phi(x)+\phi(y))^2]/2\tau - i\omega\tau} \left\{ p + i\omega - p\frac{\phi(x)-\phi(y)}{\tau} \right\} M(x,y) \\
&= \frac{p}{\pi}\,\mathrm{e}^{p(\phi(x)-\phi(y))} \left\{ (1+i\frac{\omega}{p})\mathrm{K}_0(p(1+\delta)d(x,y)) \right. \\
&\qquad \left. -(1+\delta)\frac{\phi(x)-\phi(y)}{d(x,y)}\mathrm{K}_1(p(1+\delta)d(x,y)) \right\} M(x,y),
\end{aligned}$$

where

$$\begin{aligned}
d(x,y) &\equiv \sqrt{(x-y)^2 + (\phi(x)-\phi(y))^2}, \\
M(x,y) &\equiv \left[(1+\phi'(x)^2)(1+\phi'(y)^2)\right]^{1/4}, \\
\delta &\equiv \sqrt{1+2i\frac{\omega}{p}} - 1,
\end{aligned}$$

and K_0, K_1 are modified Bessel functions. Introducing the operator

$$\hat{A}_0(\omega) \equiv -\sigma\,\partial_x \frac{1}{1+\phi'(x)^2}\partial_x + V_+(x) + \hat{\Lambda}(\omega),$$

where V_+ is the positive part of the potential, we can write the characteristic equation for the excitations of the needle crystal as

$$\hat{A}(\omega)v = \left(\hat{A}_0(\omega) - V_-\right) v = 0.$$

We are only interested in isolated zero eigenvalues of $\hat{A}(\omega)$ i.e., to excitations $v(x)$ which are (exponentially) localized near the tip of the crystal. However discretizing and truncating this equation as it stand will also produce a quasi-continuum of extended solutions corresponding to the essential spectrum of $\hat{A}$. Such solutions are clearly very

sensitive to boundary conditions i.e., to truncation effects. In particular they may very well appear as unstable modes, a phenomenon that would explain the fake instabilities found in the computation of [LM]. We avoid this problem by rewriting the last equation in term of the "Birman-Schwinger" kernel

$$Q(\omega) \equiv V_-^{1/2}\, \hat{A}_0^{-1}(\omega)\, V_-^{1/2}$$

and the modified excitation function $w \equiv V_-^{1/2}\, v$ as

$$Q(\omega) w = w \tag{3.1}$$

By theorems 4.4 and 6.2 in [P], and the analytic Fredholm theorem (see [RS]), the kernel $Q(\omega)$ is easily seen to be compact and meromorphic below the upper curve in figure 1. The only problem with this equation is the possible existence of zero eigenvalues of $\hat{A}_0(\omega)$ which would make the numerical solution of (3.1) very delicate. Fortunately both the explicit calculation of the symbol of $\hat{A}_0$ and its numerical inversion indicate that zero eigenvalues do not occur. We have thus reduced our problem to finding the eigenvalues 1 of a compact operator. Since Q is easily seen to commute with reflection at the tip of the crystal, a further reduction is obtained by restricting it to the subspaces of odd respectively even functions.

Practically we do not need to explore the entire domain Ω, but only its boundary $\partial\Omega$. In figure 3 we display the numerically computed trajectory, as ω runs around $\partial\Omega$, of the eigenvalue of $Q(\omega)$ with the largest real part. The important consequence of this figure is that 1 belongs to an unbounded open connected set disjoint from any eigenvalue of $Q(\omega)$ (for $\omega \in \partial\Omega$). Now by analytic perturbation theory, the set of all eigenvalues of $Q(\omega)$ splits into a denumerable number of finite families, each of which described by the branches of a multivalued function $\lambda(\omega)$, holomorphic on an open neighborhood of Ω. Applying the argument principle to each of these functions (in the globally uniformizing variable), we readily conclude, from the above considerations, that an eigenvalue 1 can not occur in the interior of Ω.

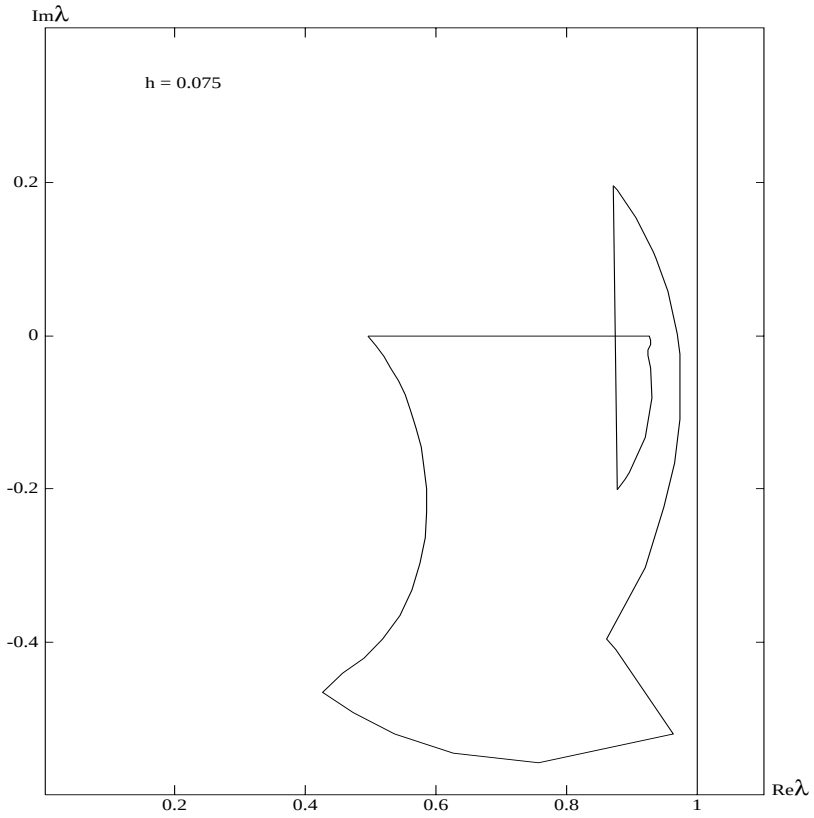

Fig. 3: the eigenvalue of $Q(\omega)$ with the largest real part as ω describes $\partial\Omega$.

4. NUMERICS.

The first step in the numerical solution of the equation (3.1) is the discretization of the operator $\hat{A}_0(\omega)$. As mentioned in the introduction, this is also the most difficult approximation to control. Given a mesh-size $h > 0$, we use the set of discretization points

$$x_j \equiv (j + \tfrac{1}{2})h \qquad j = 0, \pm 1, \pm 2, \cdots .$$

To discretize the differential operator in $\hat{A}_0$, we use the identity

$$\partial_x \frac{1}{1+x^2}\,\partial_x = \frac{1}{\sqrt{1+x^2}}\,\partial_x^2 \frac{1}{\sqrt{1+x^2}} - \frac{2x^2-1}{(1+x^2)^3},$$

and the usual three points approximation for the second derivative. Thus we get the matrix

$$\left(\partial_x \frac{1}{1+x^2}\,\partial_x\right)_{i,j} = \left[\frac{2h^{-2}}{1+x_i^2} - \frac{2x_i^2-1}{(1+x_i^2)^3}\right]\delta_{i,j} - \frac{h^{-2}}{\sqrt{(1+x_i^2)(1+x_j^2)}}\,\delta_{|i-j|,1}.$$

The potential $V_{\pm}(x)$ which is slowly varying is discretized by restriction to the mesh points. The integral operator $\hat{\Lambda}(\omega)$ needs a more careful treatment, due to the singularity of its kernel on the diagonal. We will use a numerical approximation of

$$\left(\hat{\Lambda}(\omega)\right)_{i,j} = \lim_{\epsilon \downarrow 0} \int_{\epsilon<|u|<h/2} \hat{\Lambda}(\omega; x_i, x_j + u)\, du. \tag{4.1}$$

The first problem we are faced with is the evaluation of the modified Bessel functions in the sector $\{|\arg z| < \pi/4\}$. For that purpose we note that for fixed ω in the lower half-plane, the argument $z = p(1+\delta)d(x,y)$ of K_0 and K_1 lie on a fixed ray $\{\arg z = \theta\}$ which we divide in seven sub-intervals:

$$\begin{aligned}
I_1 &= \{|z| \in [0, 2.2\,10^{-305}[\},\\
I_2 &= \begin{cases} \{|z| \in [2.2\,10^{-305}, 3.0\,10^{-9}[\} & \text{for } K_0,\\ \{|z| \in [2.2\,10^{-305}, 7.9\,10^{-10}[\} & \text{for } K_1, \end{cases}\\
I_3 &= \begin{cases} \{|z| \in [3.0\,10^{-9}, 1[\} & \text{for } K_0,\\ \{|z| \in [7.9\,10^{-10}, 1[\} & \text{for } K_1, \end{cases}\\
I_4 &= \{|z| \in [1, 2[\},\\
I_5 &= \{|z| \in [2, 6[\},\\
I_6 &= \{|z| \in [6, 705[\},\\
I_7 &= \{|z| \in [705, \infty[\}.
\end{aligned}$$

Evaluation on the first interval results in a fatal error. On the second interval we use the $\mathrm{O}(z)$ approximation around 0 (see [BAT]):

$$\begin{aligned}
K_0(z) &\approx \gamma - \log(z/2),\\
K_1(z) &\approx \frac{1}{z}.
\end{aligned}$$

On the third interval, uniform (ω independent) approximations

$$\begin{aligned}
K_0(z) &\approx A_0(2z^2-1) - \log(z) B_0(2z^2-1),\\
K_1(z) &\approx \frac{1}{z} + z\left(A_1(2z^2-1) + \log(z) B_1(2z^2-1)\right),
\end{aligned}$$

are used. The polynomials $A_\nu(t)$ and $B_\nu(t)$ are taken from the NAG library (routine S18ACF expansion 0038 and routine S18ADF expansion 0046). On the fourth and fifth intervals, uniform polynomial approximations of the form

$$K_\nu(z) \approx \mathrm{e}^{-z} P_{\nu,\omega}(|z|)$$

are generated by the Remez algorithm (see its description in [L], for example), on the basis of the rapidly convergent integral formulae (see [BAT])

$$K_0(z) = \int_0^\infty \mathrm{e}^{-z\mathrm{ch}(t)}\, dt,$$
$$K_1(z) = \int_0^\infty \mathrm{ch}(t)\mathrm{e}^{-z\mathrm{ch}(t)}\, dt.$$

On the sixth interval, we use the well known asymptotic expansions (see [BAT]), while on the last interval we simply set the Bessel functions to zero. All numerical integrations are performed by a robust adaptive integrator of degree 30 based on the 15 points Gauss quadrature formula. The off-diagonal elements of the discretized integral operator are simply computed by numerical integration since the integrand in formula (4.1) is smooth. On the diagonal however we remove the singularity of the integrand at $u = 0$ by rewriting

$$\left(\hat{\Lambda}(\omega)\right)_{i,i} = \int_0^{(h/2)^{1/M}} \left\{\hat{\Lambda}(\omega; x_i, x_i + u^M) + \hat{\Lambda}(\omega; x_i, x_i - u^M)\right\} M u^{M-1} du$$

for some $M > 2$. We have thus achieved, in principle, the discretization of the operator $\hat{A}_0$, producing an infinite matrix $\hat{a}_0^{(h)}$.

To take into account the reflection symmetry around the tip, we further introduce the reduced matrices

$$\left(\hat{a}_0^{(h,\pm)}\right)_{i,j} \equiv \left(\hat{a}_0^{(h)}\right)_{i,j} \pm \left(\hat{a}_0^{(h)}\right)_{i,-j-1},$$

indexed by $i, j = 0, 1, 2, 3, \cdots$. As indicated in the introduction, we only consider the symmetric sector i.e., the matrix $\hat{a}_0^{(h,+)}$.

In practice, of course, we introduce a spatial cutoff by only computing a finite $N \times N$ square matrix $\hat{a}_0^{(h,N,+)}$. To keep the errors introduced by this truncation under control, we always use values of N which are so large that the final results of the computation i.e., the eigenvalues of the matrix

$$\left(q^{(h,N,+)}\right)_{i,j} \equiv \sqrt{V_-(x_i)} \left(\frac{1}{\hat{a}_0^{(h,N,+)}}\right)_{i,j} \sqrt{V_-(x_j)}$$

approximating the Birman-Schwinger kernel Q, becomes independent of N. We also check the eigenfunctions corresponding to eigenvalues close to 1 to be sure that they vanish before reaching the spatial cutoff $x_{\max} = (N - \frac{1}{2})h$.

The inversion in the above formula is carried out by the Crout LU-decomposition algorithm with pivoting described in [WR-1]. The same is used to compute the linear response function which we define to be

$$u^{(h,N,+)}(\omega; x_i) \equiv \left((\hat{a}_0^{(h,N,+)}(\omega) - V_-)^{-1} \right)_{i,1} .$$

Thus figure 2 is in fact a plot of the function

$$\alpha(\omega) \equiv \log_{10} \left(\max_{0 \le i < N} \left| u^{(h,N,+)}(x_i) \right| \right)$$

computed at $h = 0.075$.

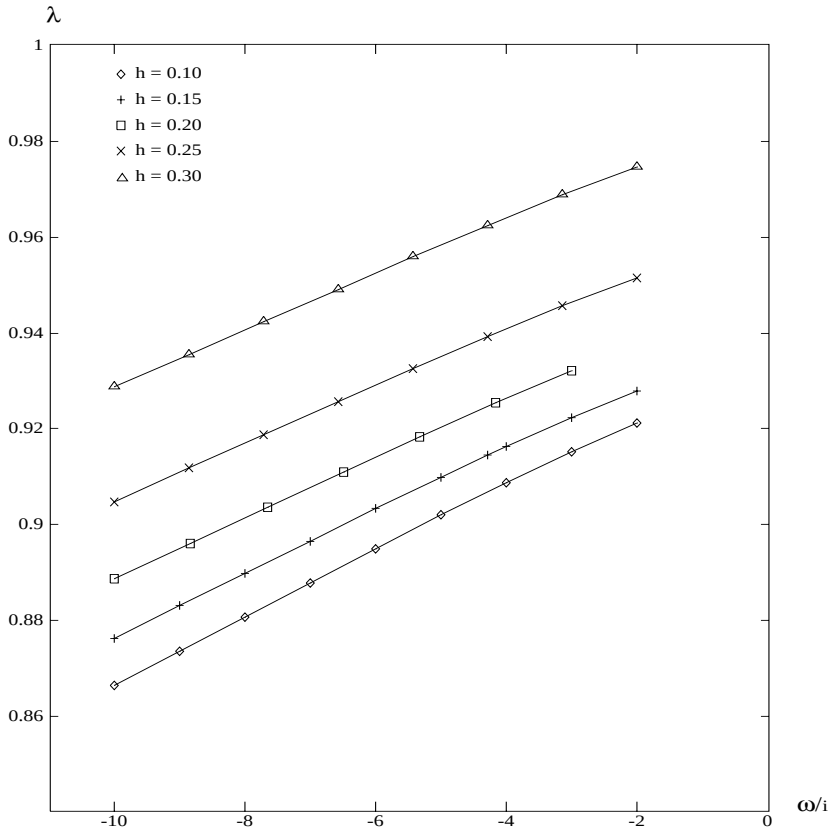

Fig. 4: the eigenvalue with largest real part for imaginary ω.

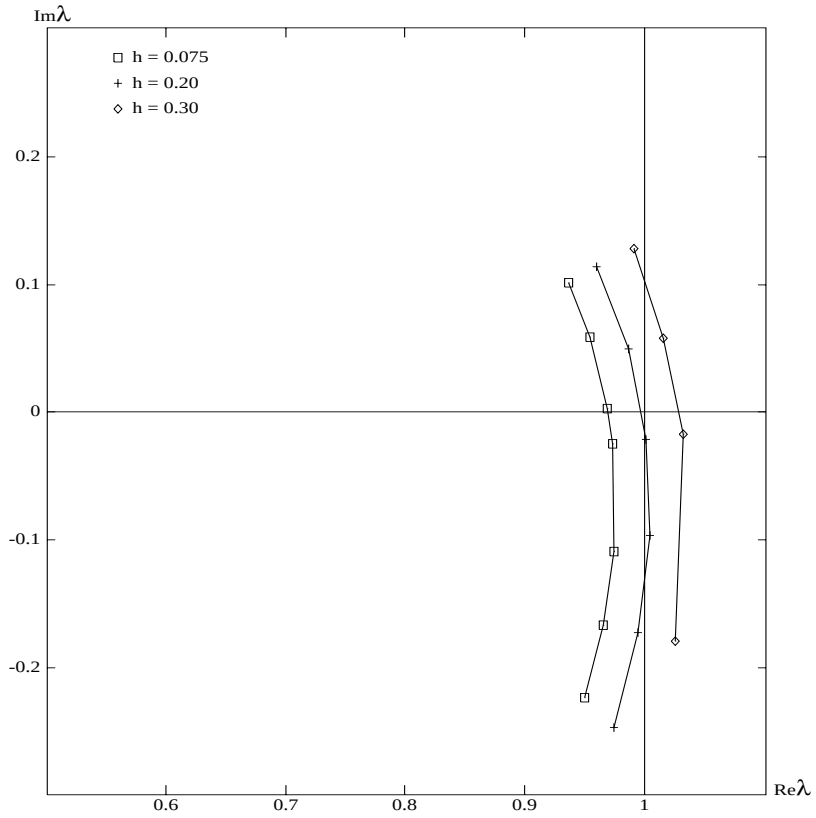

Fig. 5: the eigenvalue with largest real part near the point of closest approach to 1.

We now have to diagonalize the matrix $q^{(h,N,+)}(\omega)$. For that purpose we first perform the balancing proposed in [WR-2] to reduce subsequent numerical errors. The balanced matrix is then transformed to upper-Hessenberg form with the *comhes* algorithm described in [WR-3]. Finally this Hessenberg matrix is put into triangular form by the LR-algorithm using the *comlr2* routine of [WR-4]. From this triangular matrix eigenvalues and eigenvectors of the original Birman-Schwinger operator are constructed. The figure 3 represent the trajectory $\lambda(\omega)$, as ω runs around the boundary of Ω, of the eigenvalue of $q^{(h,N,+)}(\omega)$ with the largest real part, computed at $h = 0.075$.

To control the continuum limit $h \to 0$, we studied the h-dependence of the eigenvalues of $q^{(h,N,+)}$ in the two critical cases where they may approach 1 as $h \downarrow 0$. In figure 4 we consider purely imaginary ω and display the eigenvalue with the largest real part, which turns out to be real, as a function of ω/i for various values of h. One can see from this figure that the distance of the spectrum to 1 increases as $h \downarrow 0$, which is a good indication that the continuum limit is well behaved. The same conclusion can be drawn

from figure 5 where the eigenvalue with largest real part has been ploted for values of $\omega \in \partial\Omega$ near the point of closest approach to 1.

5. REFERENCES

[BBL] M. Barber, A. Barbieri and J. S. Langer: Dynamics of Dentritic Sidebranching in the Two Dimensional Symmetric Model of Solidification. Phys. Rev. A **36**, 3340 (1987).

[KL] D. Kessler and H. Levine: Stability of Dentritic Crystals. Phys. Rev. Lett. **57**, 3069-3072 (1986).

[LM] J. S. Langer and H. Müller-Krumbhaar: Theory of Dentritic Growth 3: Effects of Surface Tension. Acta Metall. **29**, 145 (1981).

[BPS] D. Bensimon, P. Pelcé and B. I. Shraiman: Dynamics of Curved Fronts and Pattern Selection. J. de Physique **48**, 2081-2087 (1987).

[P] C.-A. Pillet: Stabilization of Needle-Crystals by the Gibbs-Thomson Effect. (To appear).

[BAT] H. Bateman et al.: *Higher Transcendental Functions*, McGraw-Hill, NY (1953).

[L] P.-J. Laurent: *Approximation et optimisation*, Hermann, Paris (1972).

[WR] J. H. Wilkinson and C. Reinsh: *Linear Algebra*, Springer, Berlin Heidelberg New-York (1971).

[WR-1] H. J. Bowdler, R. S. Martin, G. Peters and J. H. Wilkinson: Solution of Real and Complex Systems of Equations. In [WR]

[WR-2] B. N. Parlett and C. Reinsch: Balancing a Matrix for Calculation of Eigenvalues and Eigenvectors. In [WR]

[WR-3] R. S. Martin and J. H. Wilkinson: Similarity Reduction of a General Matrix to Hessenberg Form. In [WR]

[WR-4] G. Peters and J. H. Wilkinson: Eigenvectors of Real and Complex Matrices by LR and QR Triangularizations. In [WR]

[LT] J. S. Langer and L. A. Turski: Studies in the Theory of Interfacial Instability 1: stationnary Symmetric Model. Acta Metall. **25**, 1113 (1977).

[RS] M. Reed and B. Simon: *Analysis of Operators*, Academic Press, New York (1978).